

Cell Reports, Volume 34

Supplemental information

**Mapping of the contraction-induced phosphoproteome
identifies TRIM28 as a significant regulator
of skeletal muscle size and function**

Nathaniel D. Steinert, Gregory K. Potts, Gary M. Wilson, Amelia M. Klamen, Kuan-Hung Lin, Jake B. Hermanson, Rachel M. McNally, Joshua J. Coon, and Troy A. Hornberger

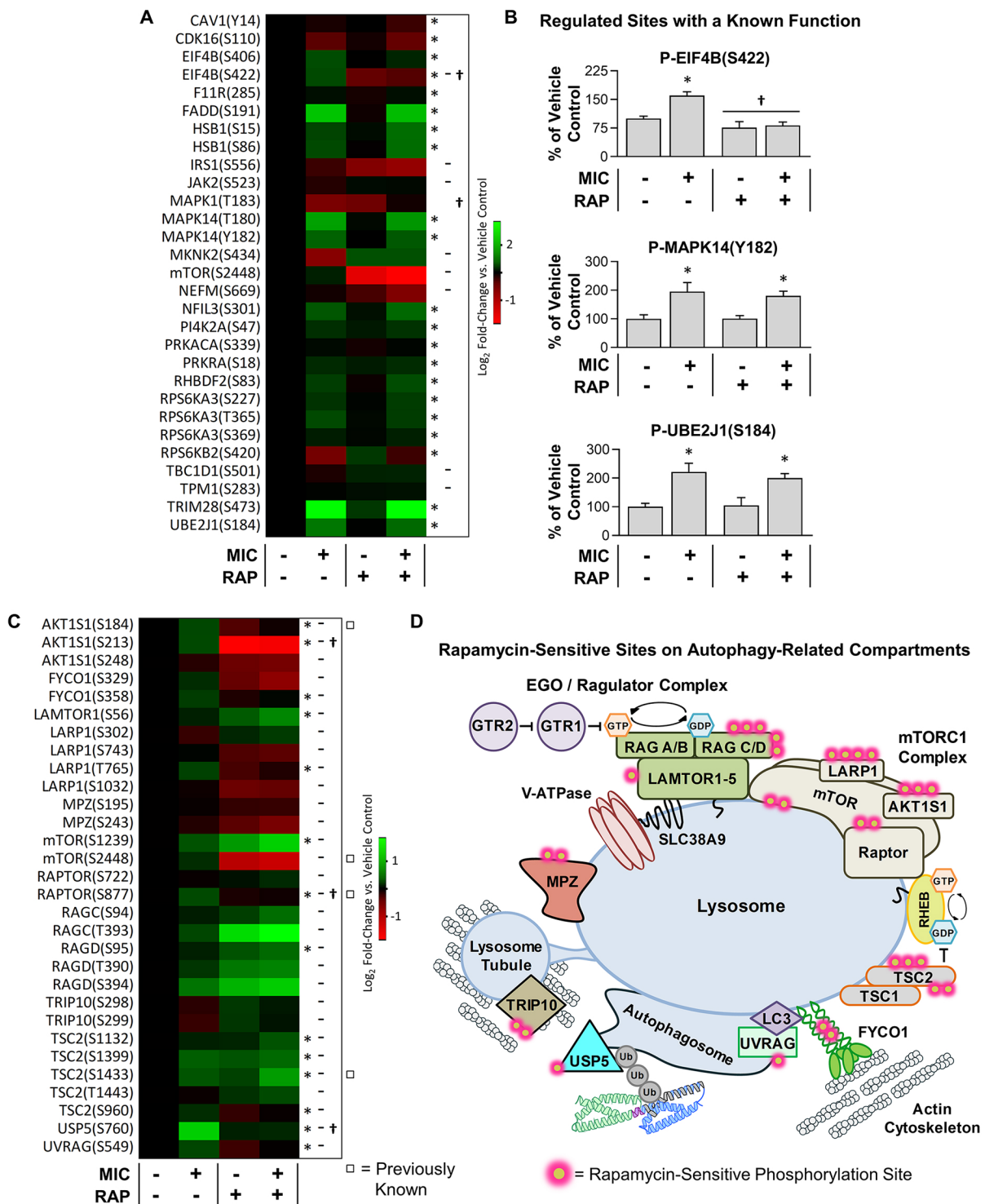


Figure S1. Representative features of the rapamycin-sensitive and maximal-intensity contraction regulated phosphoproteome (Relates to figures 1 and 2). Mouse TA muscles were subjected to the workflow described in Figure 1. **(A)** Heatmap of the phosphorylation state of sites with a known regulatory function that revealed a main effect for maximal-intensity contractions (MIC), a main effect for rapamycin (RAP), and / or an interaction between MIC and RAP. Horizontal bar indicates a significant effect for RAP, * significant effect of MIC, † significant interaction between RAP and MIC, $P < 0.05$. **(B)** Graphs for three of the sites listed in A, values represent the group mean + SEM, $n = 4-6$ / group. **(C)** Heatmap of the phosphorylation state on sites that revealed a main effect for rapamycin and were annotated with autophagy-related cellular compartments (Gtr1-Gtr2 GTPase complex, TORC1 complex, EGO complex, and / or the lysosome). **(D)** Schematic which illustrates various proteins contained within the complexes described in C, as well as the proteins that exhibited a rapamycin-sensitive alteration in their phosphorylation state. Note: only 4 of the identified phosphorylation sites within this group were previously known to be rapamycin-sensitive.

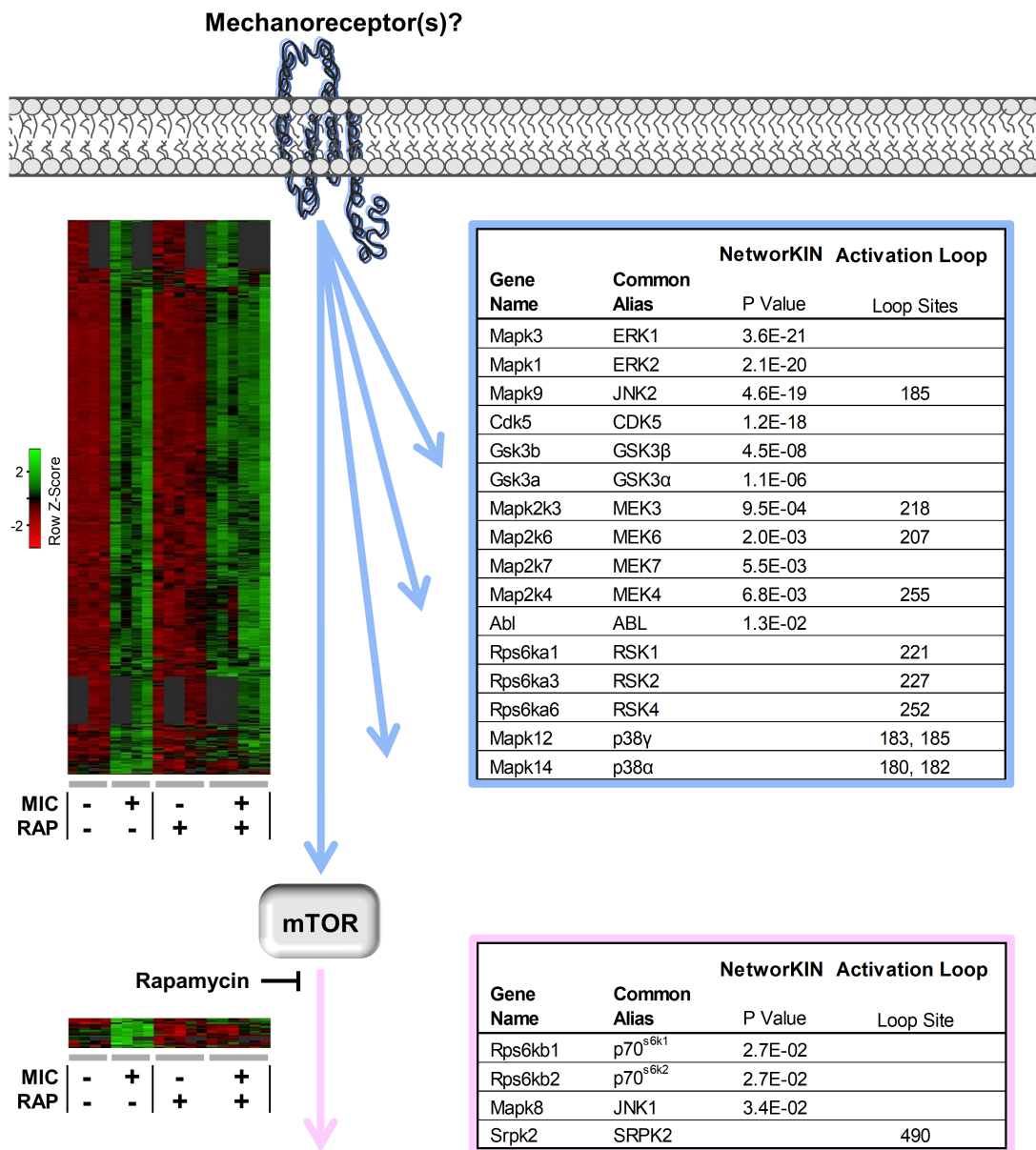


Figure S2. Prediction of the kinases that are activated by maximal-intensity contractions and their sensitivity to rapamycin (Relates to figure 1 and 2). Mice were subjected to the workflow described in Figure 1. The heatmap at the top displays the phosphopeptides that revealed a significant main effect for maximal-intensity contractions (MIC), as well as a significant MIC-induced increase in phosphorylation within the vehicle group (FDR corrected moderated t-test $P < 0.05$). The heatmap at the bottom displays phosphopeptides that revealed significant interaction between MIC's and rapamycin, as well as a significant MIC-induced increase in phosphorylation within the vehicle group (FDR corrected moderated t-test $P < 0.05$). Within these subgroups, NetworkKIN, and the presence of activation loop phosphorylation events, were used to predict which kinases had been activated (P values for the NetworkKIN results were derived from an FDR corrected Kolmogorov-Smirnov test). The kinases identified for the interaction subgroup were filtered so that only the kinases identified in the MIC main effect subgroup were retained (pink box), and then these kinases were removed from the list of kinases identified for the MIC main effect subgroup (blue box). The resulting lists describe the MIC-regulated kinases that are predicted to be activated upstream and / or parallel to the rapamycin-sensitive elements of mTOR (blue), versus those which are predicted to be activated downstream of the rapamycin-sensitive elements of mTOR (pink).

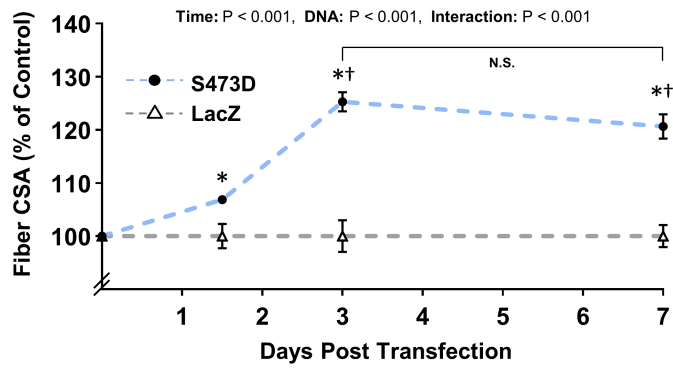


Figure S3. Time-course of the hypertrophic effects of S473 phosphomimetic TRIM28 (Relates to figure 4). Electroporation was used to transfect the myofibers of wild-type C57BL6 mouse tibialis anterior muscles with plasmid DNA encoding HA-tagged phosphomimetic TRIM28 (S473D), or LacZ as a control condition. The muscles were collected at 1.5, 3 or 7 days post-transfection, and then the cross-sectional area (CSA) of the transfected and non-transfected myofibers in each muscle was measured. The transfected to non-transfected myofiber size ratios were calculated and expressed relative to the mean of the time-matched LacZ control samples. Values are reported as the group mean + SEM, n = 4-5 muscles / group (180-549 transfected and 811-1419 non-transfected myofibers / group). The data was analyzed with two-way ANOVA followed by Student-Newman-Keuls post hoc analyses. Significant difference versus: * time-matched LacZ, † 1.5 day TRIM28(S473D), P < 0.05. N.S. indicates no significant difference.

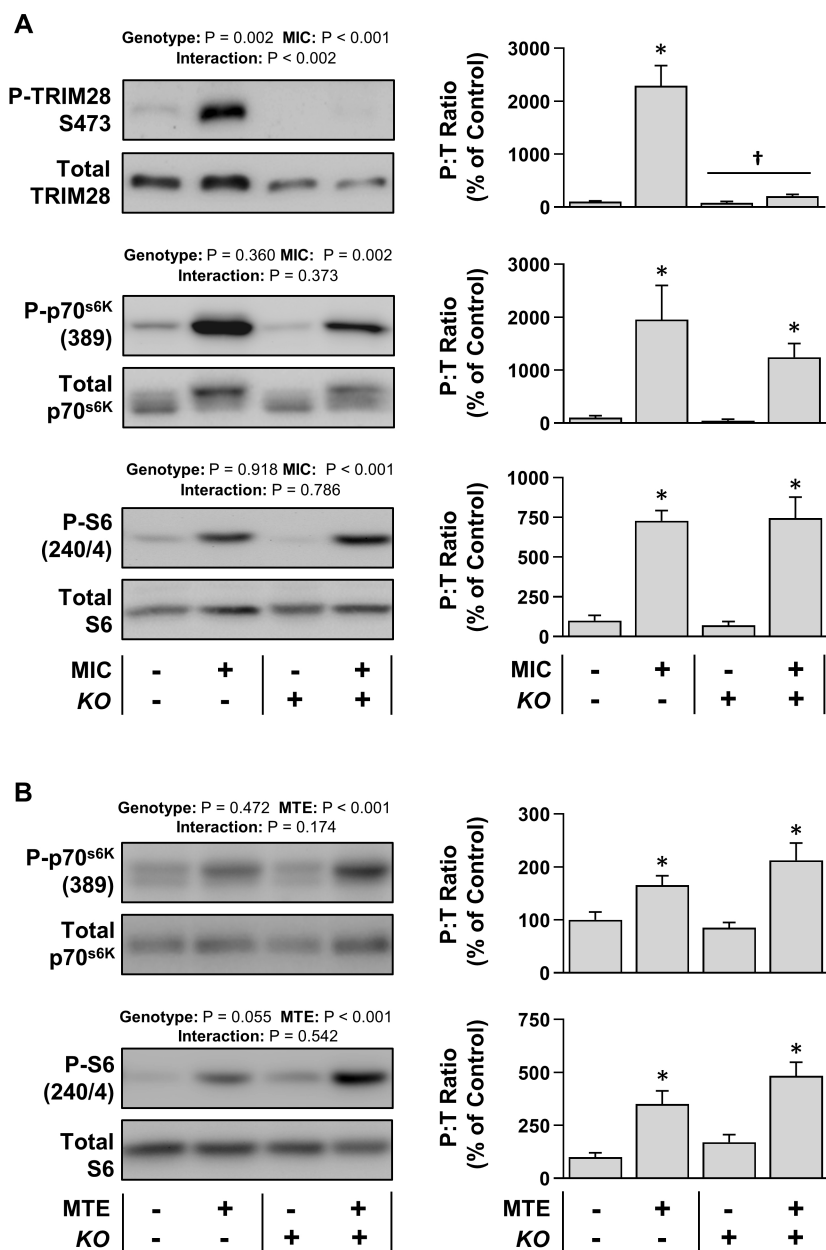


Figure S4. TRIM28 is not required for the mechanical activation of RSmTOR signaling (Relates to figure 6). TRIM28 knockout mice (KO^+) and their control littermates (KO^-) were treated with tamoxifen for 5 days. At 14 days post tamoxifen the animals were subjected to one of the following procedures: **(A)** The Tibialis anterior (TA) muscles were subjected to a bout of maximal-intensity contractions (MIC+) or the control condition (MIC-). The mice were allowed to recover for 1 hr and then their TA muscles were subjected to western blot analysis for phosphorylated (P) and total (T) TRIM28, as well as markers of RSmTOR signaling (P-p70^{s6K} and P-S6). **(B)** The plantaris (PLT) muscles were subjected to MTE or a sham surgery. The mice were then allowed to recover for 90 min and then their PLT muscles were analyzed for the same markers of RSmTOR signaling as in A. Values in the graphs represent the group means \pm SEM, $n = 5-12$ / group. The results in A were analyzed with two-way repeated measures ANOVA followed by Student-Newman-Keuls post hoc analyses, and the results in B were analyzed by regular two-way ANOVA followed by Student-Newman-Keuls post hoc analyses. Horizontal bar indicates a significant effect of genotype, $P < 0.05$, * indicates a significant effect of MIC or MTE, $P < 0.05$, and † indicates a significant interaction between genotype and MIC / MTE

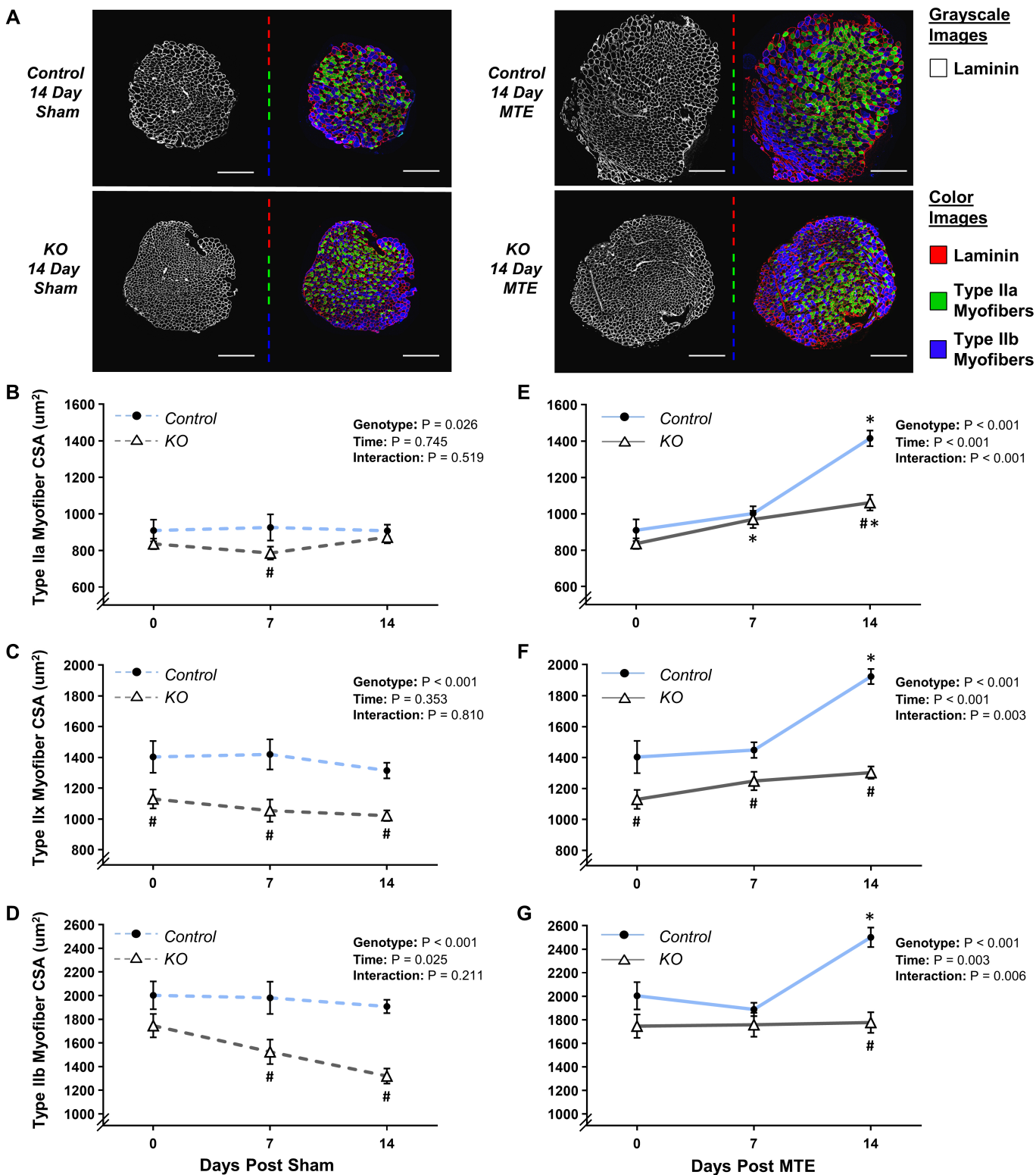


Figure S5. The loss of TRIM28 exerts myofiber type specific effects on size and mechanical load-induced hypertrophy (Relates to figure 6). TRIM28 knockout mice (*KO*) and their control littermates were treated with tamoxifen for 5 days and, at 14 days post tamoxifen, their PLT muscles were subjected to MTE or a sham surgery. After 0, 7, or 14 days of recovery, mid-belly cross-sections of the PLT muscles were subjected to IHC for laminin and myofiber type identification. (A) Representative images of cross-sections that were stained for laminin, type IIa, and type IIb myofibers, scale bars = 400 μm . (B-G) The average CSA of each myofiber type (i.e., type IIa, IIx, and IIb) per muscle was determined. Values in the graphs represent the group mean \pm SEM, $n = 9-14$ muscles / group (552-1292 myofibers / group). The data in B-G was analyzed with two-way ANOVA followed by Student-Newman-Keuls post hoc analyses. Significantly different from: # the time matched control genotype, * day 0 within a given genotype, $P < 0.05$.

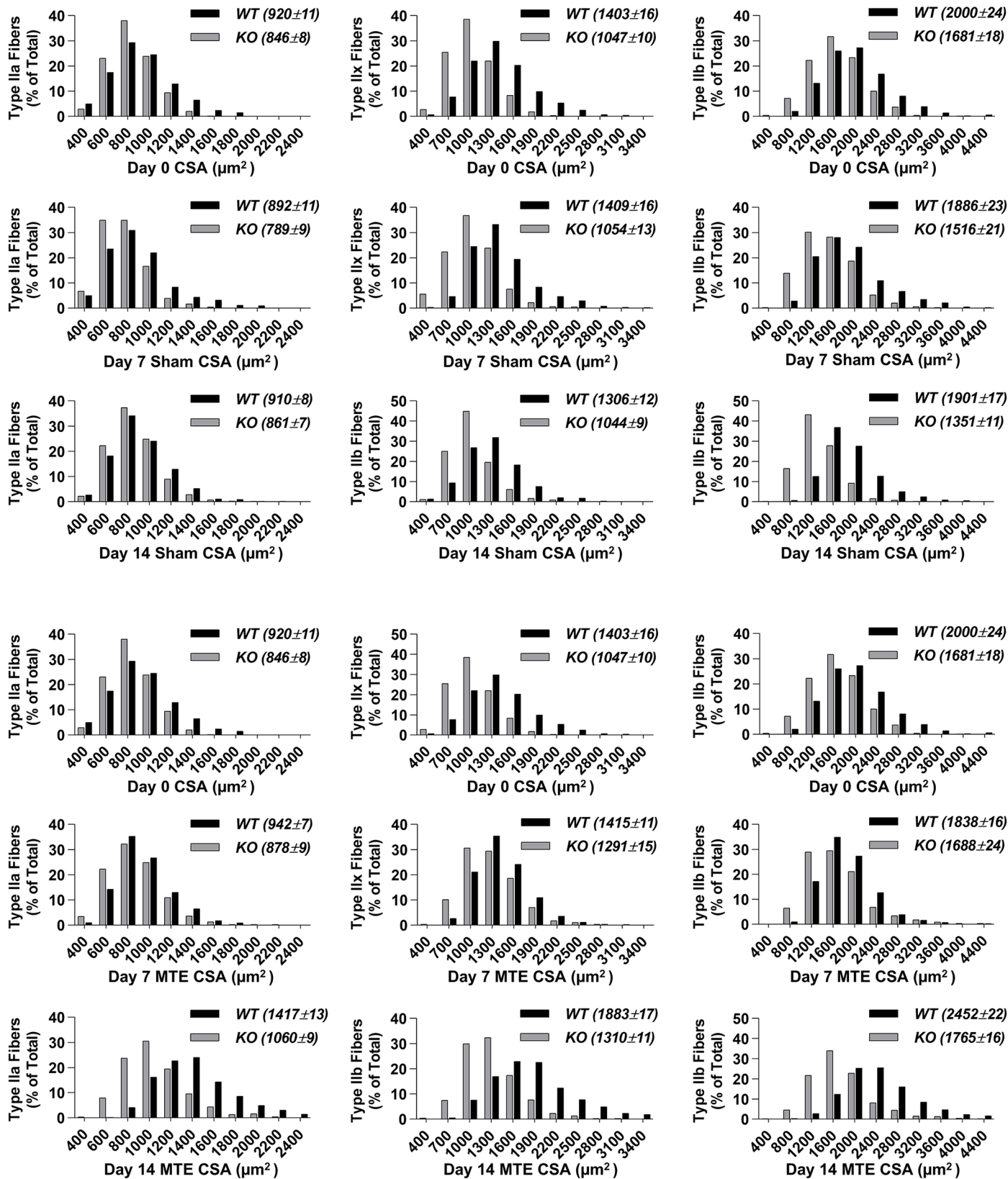


Figure S6. The loss of TRIM28 exerts myofiber type specific effects on size and mechanical load-induced hypertrophy (Relates to figure 6). (A) Frequency histograms of the data presented in Figure S5B-D. (B) Frequency histograms of the data presented in Figure S5E-G. Values in the graphs represent the group mean \pm SEM, $n = 9-14$ muscles / group (552-1292 myofibers / group).

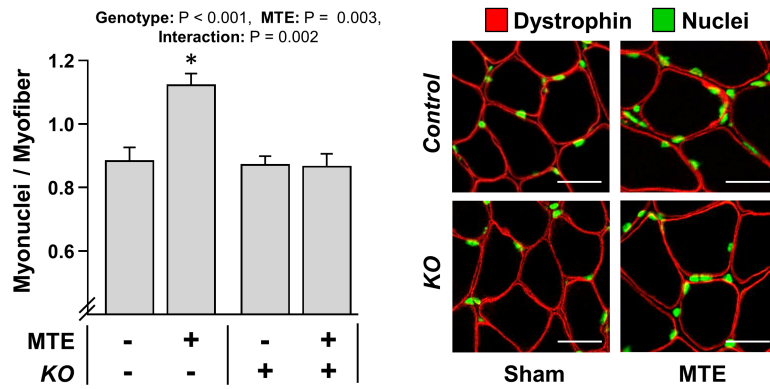


Figure S7. TRIM28 is required for the myotenyctomy-induced accretion of myonuclei (Relates to figure 6). TRIM28 knockout mice (KO^+) and their control littermates (KO^-) were treated with tamoxifen for 5 days and, at 14 days post tamoxifen, their PLT muscles were subjected to myotenyctomy (MTE+) or a sham surgery (MTE-). After 14 days of recovery, mid-belly cross-sections of the PLT muscles were subjected to immunohistochemistry for dystrophin and Hoechst to identify nuclei, scale bars = 25 μm . The resulting images were used to quantify of the number of myonuclei per myofiber. Values represent the group mean + SEM, $n = 4-7$ / group (1358-1945 myofibers / group). The data was analyzed with two-way ANOVA followed by Student-Newman-Keuls post hoc analyses. * Significant effect of MTE, $P < 0.05$.